Adsorption (2007) 13: 257–265
DOI 10.1007/s10450-007-9023-7

Synthesis and adsorption investigations of zeolites MCM-22 and MCM-49 modified by alkali metal cations

Justyna Pawlesa · Arnošt Zukal · Jiří Čejka

Received: 1 May 2007 / Revised: 4 July 2007 / Accepted: 11 July 2007 / Published online: 20 September 2007

Abstract Ion exchange was made on MCM-22 and MCM-49 zeolites with different Si/Al molar ratios, with Li^+, Na^+, K^+, and Cs^+ ions and the study of the influence of alkali metal cations on CO_2 adsorption properties was performed. The degree of ion-exchange decreased for larger cations (Cs^+) apparently due to steric hindrances. The exchange with different cations led to a decrease in the surface area and the micropore volume. Our study shows that the adsorption capacity of the tested zeolites depends significantly on the nature and the concentration of the charge-compensating cations. The highest CO_2 adsorption capacity was obtained on the MWW zeolites with the lowest Si/Al molar ratio and the Li^+ or K^+ cations.

Keywords MCM-22 zeolite · MCM-49 zeolite · Alkali metal cation exchange · N_2 and CO_2 adsorption

Abbreviations

S_{BET}	BET surface area, m^2/g
$S_{external}$	external surface area, m^2/g
V_{total}	total pore volume, cm^3/g
V_{micro}	micropore volume, cm^3/g
K_H	Henry's constant, cm^3/g STP

1 Introduction

Zeolites represent the most important group of inorganic microporous materials with molecular sieve properties. Their ordered pore structure makes them useful in the broad range of industrial application widespread from detergents, catalysts up to adsorbents (Tanabe and Hölderich 1999; Čejka and Wichterlová 2002).

MCM-22 is a novel molecular sieve that crystallizes as aggregates of thin sheets or platelets, and has an unusual crystal structure (Rubin and Chu 1990). Its framework topology is comprised of two independent pore systems, both accessible through 10-membered rings. One of these pore systems is defined by two-dimensional sinusoidal channels, which maintain 10-ring diameter throughout the structure. The other consists of large supercages whose inner free diameter, 0.71 nm, is defined by 12 rings with an inner height of 1.82 nm (Leonowicz et al. 1994; Dorset et al. 2005). MCM-49 molecular sieve exhibits XRD pattern nearly identical with that for MCM-22 but with subtle, distinct differences in peak positions and intensities (Dorset 2003; Lawton et al. 1996). These differences can be explained by different synthesis procedures, while MCM-49 is prepared by direct hydrothermal synthesis, MCM-22 is at first prepared as layered precursor and three-dimensional structure is formed during the following calcination. The general similarities in the XRD patterns suggest that the framework topology of MCM-49 is isostructural with that of MCM-22. However, MCM-49 generally has a lower Si/Al ratio than MCM-22 (Kennedy et al. 1999; Santos Marques et al. 1999).

While catalytic properties of MCM-22 zeolite have been investigated in a number of reactions (Corma and Martínez-Triguero 1997; Čejka et al. 2002; Ravishankar and Sivasanker 1996), detailed adsorption studies are still missing. This is despite the fact that the structural features of MCM-22/MCM-49 zeolites make this MWW materials family especially appealing for characterization studies. MCM-49 contains more aluminum in the framework

J. Pawlesa · A. Zukal (✉) · J. Čejka
J. Heyrovský Institute of Physical Chemistry of ASCR v.v.i.,
Dolejškova 3, 182 23 Prague 8, Czech Republic
e-mail: arnost.zukal@jh-inst.cas.cz

than MCM-22; hence, MCM-49 should also contain more cations than MCM-22. The concentration of cations and their type influence the electric field inside the pores, as well as the available pore volume. Cations are preferred adsorption sites that are especially important for interacting with polar or easily polarizable molecules (Kučera et al. 2004). Therefore, the extent or strength of adsorption of molecules in zeolitic pores can be dominated by interactions of the adsorbate with the electric field induced by the cations.

Carbon dioxide is a prominent molecule for a systematic investigation of the influence of the cations on the adsorption properties of zeolites because it possesses a quadrupole moment. The adsorption of CO_2 has been most frequently studied on ion-exchanged zeolites A, X, and Y (Delaval and De Lara 1981; Shiralkar and Kulkarni 1984; Siriwardane et al. 2001; Maurin et al. 2005; Plant et al. 2006; Walton et al. 2006). However, there has not been a systematic investigation of CO_2 adsorption on both MCM-22 and MCM-49 zeolites containing alkali metal cations from Li^+ to Cs^+.

In this contribution we report on the study of the synthesis and adsorption properties MCM-22/MCM-49 zeolites. The structural parameters of prepared materials containing Li^+, Na^+, K^+, and Cs^+ cations were evaluated using X-ray powder diffraction (XRD) and nitrogen adsorption at −196°C. Particle morphology was determined by scanning electron microscopy (SEM), chemical composition of MCM-22/MCM-49 zeolites was determined by X-ray fluorescence spectroscopy (XRF). An investigation of the effect of alkali metal substitution on adsorption properties of zeolites under study was performed by means of measurement of CO_2 adsorption at 0°C.

2 Experimental

Series of MCM-22 and MCM-49 zeolites with different Si/Al ratios and different molar ratios of the organic cation (R_o) to the inorganic cation (R_i) have been synthesized (Table 1). The sodium aluminate (50–56% Al_2O_3, 40–45% Na_2O, Riedel-de Haën) and Cab-O-Sil M5 (Cabot GmbH) have been used as a source of aluminum and silicon, respectively. In all experiments, hexamethyleneimine (HMI, Aldrich) was employed as a structure directing agent. More specifically the MCM-22 sample with Si/Al = 15 and R_o/R_i = 3.5 was prepared in the following way: 0.84 g of $NaAlO_2$ and 0.54 g of NaOH were dissolved in 125.0 g of H_2O, and then, 8.6 g of HMI and 9.2 g of Cab-O-Sil M5 were added to this solution while stirring. After 60 min of stirring the resulting gel was introduced into 250 ml Teflon lined stainless-steel autoclaves. The crystallization took place under agitation for 5 days at 150°C.

The solid product was washed out with distilled water until pH < 9 and then dried overnight at 100°C. The removal of the template was performed by calcination in air for 6 h at 540°C with a temperature ramping rate of 1°C/min. Calcined samples were subsequently converted into alkali ion forms by treatment with 1.0 M MNO_3 water solutions (M = Na^+, K^+, Cs^+) or LiCl in the case of Li^+ form (100 mL/1 g of zeolite). For this purpose 100 mL of the solution was used per 1 g of the sample. The procedure was repeated two times and each step took 8 h at 60°C. During ion exchange modification the pH values of the ion exchange suspensions were adjusted to the value of 9 with a 0.5 M MOH or LiOH solutions.

All as-synthesized, calcined and ion-exchanged samples were checked for their crystallinity and phase purity by X-ray powder diffraction on a Bruker D8 X-ray powder diffractometer equipped with a graphite monochromator and

Table 1 Synthesis conditions of MWW zeolite with different initial Si/Al molar ratio and different molar ratio of organic (R_o) to inorganic cation (R_i)

Sample	Molar composition of initial gel $Na_2O : Al_2O_3 : SiO_2 : HMI : H_2O$	Si/Al_{gel}	R_o/R_i	Product
S001	0.052 : 0.038 : 1 : 0.56 : 45.38	10	2.9	MCM-22 + amorph.
S002	0.047 : 0.049 : 1 : 0.56 : 45.38	12	3.1	MCM-22 + amorph.
S003	0.047 : 0.033 : 1 : 0.56 : 45.38	15	3.5	MCM-22
S004	0.047 : 0.047 : 1 : 0.56 : 45.38	20	3.9	MCM-22
S005	0.047 : 0.016 : 1 : 0.56 : 45.38	30	4.4	MCM-22
S006	0.047 : 0.012 : 1 : 0.56 : 45.38	40	4.7	MCM-22
S007	0.047 : 0.098 : 1 : 0.56 : 45.38	50	4.9	MCM-35
S008	0.093 : 0.043 : 1 : 0.56 : 45.38	15	2.5	MCM-49
S009	0.120 : 0.043 : 1 : 0.56 : 45.38	15	2.0	MCM-49 + ferierite
S010	0.129 : 0.043 : 1 : 0.56 : 45.38	15	1.9	MCM-49 + mordenite
S011	0.147 : 0.043 : 1 : 0.56 : 45.38	15	1.75	mordenite

position sensitive detector (Våntec-1) using CuKα radiation (at 40 kV and 30 mA) in Bragg-Brentano geometry. The size and shape of synthesized materials were evaluated by scanning electron microscopy images using a JEOL JSM-5500LV instrument. To estimate the chemical composition of synthesized zeolites and their ion-exchange forms the X-ray fluorescence spectroscopy (Philips PW 1404) was employed.

Nitrogen and carbon dioxide supplied by Messer (Griesheim, Germany) were used as adsorptives. Adsorption isotherms of nitrogen at −196°C (i.e. 77.35 K) and carbon dioxide at 0°C (i.e. 273.15 K) on zeolites under study were determined using an ASAP 2020 (Micromeritics) static volumetric apparatus. In order to attain a sufficient accuracy in the accumulation of the adsorption data, this instrument is equipped with pressure transducers covering the 133 Pa, 1.33 kPa and 133 kPa ranges.

Before each adsorption measurement the sample was outgassed using a special heating program allowing for a slow removal of most preadsorbed water at low temperatures. This was done to avoid potential structural damage of the sample due to surface tension effects and hydrothermal alternation. Starting at ambient temperature the sample was outgassed at 110°C (temperature ramp of 0.5°C/min) until the residual pressure of 0.5 Pa was obtained. After further heating at 110°C for 1 h the temperature was increased (temperature ramp of 1°C/min) until the temperature of 250°C was achieved. This temperature was maintained for 8 h.

3 Results and discussion

X-ray powder diffraction patterns of the MCM-22 materials (Fig. 1) confirmed good crystallinity of the obtained MCM-22 zeolites with Si/Al molar ratio between 15 and 40. For Si/Al lower than 15 we observed a decreasing intensity of the main diffraction lines characteristic for MCM-22 structure. The attempt to increase Si/Al molar ratio in the synthesis gel to the value of 50 led to the formation of MCM-35 (Barrett et al. 1999), which does not belong to MWW family of zeolites (Fig. 1).

In the range of Si/Al from 15 to 40 we did not observe any changes in the intensities and line widths of the diffraction lines for all as-synthesized as well as calcined MCM-22 zeolites. Therefore, we can conclude that there is no significant influence of the Si/Al ratio in the initial gels as well as in the final products on the resulting crystallinity of the final product. This conclusion is in good agreement with the data of scanning electron microscopy. SEM micrographs of the synthesized samples show typical morphology for MWW material (Corma et al. 1995), mostly forming sheets like discs or agglomerates of several cross-linked discs. It is seen that the resulting crystal size of ∼1 μm and crystal morphology in

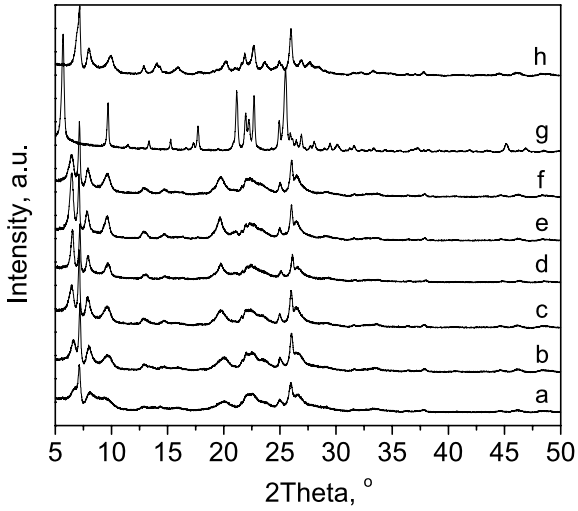

Fig. 1 X-ray diffraction patterns of the as-made MWW samples with different Si/Al molar ratio in the initial gel and different molar ratio of organic (R_o) to inorganic cation (R_i): *a*, Si/Al = 10, R_o/R_i = 2.9 (sample S001); *b*, Si/Al = 12, R_o/R_i = 3.1 (sample S002); *c*, Si/Al = 15, R_o/R_i = 3.5 (sample S003); *d*, Si/Al = 20, R_o/R_i = 3.9 (sample S004); *e*, Si/Al = 30, R_o/R_i = 4.4 (sample S005); *f*, Si/Al = 40, R_o/R_i = 4.7 (sample S006); *g*, Si/Al = 50, R_o/R_i = 4.9 (MCM-35); *h*, Si/Al = 15, R_o/R_i = 2.5 (sample S008)

the case of MCM-22 zeolite are not influenced by the initial Si/Al molar ratio (Fig. 2).

MCM-22 is synthesized when the molar ratios of the organic template (R_o) to the inorganic cations (R_i) is higher than 2.5. For R_o/R_i ratio around 2.5, MCM-49 can be obtained as a pure phase with good yields (Fig. 1). MCM-49 is isostructural zeolite with MCM-22, which is prepared directly by hydrothermal synthesis without formation of layered precursor in contrast to the synthesis of MCM-22 (Roth 2005). For lower R_o/R_i ratios the samples obtain impurities like ferrierite and/or mordenite (for R_o/R_i under 1.75). MCM-49 can be obtained in very narrow range of Si/Al molar ratio.

When the initial molar ratio of organic cations to inorganic cations is higher than 3.0, which is the case of MCM-22 materials, the molar ratios of Si/Al in the initial gel correspond well to Si/Al ratios obtained in the product (Table 2). In the case of the zeolite MCM-49 it was observed that by increasing the concentration of alkali metal cations in the initial gel lower amount of silicon is incorporated into its framework than in the case of MCM-22 (Table 2).

The XRD patterns of the ion-exchanged materials correspond well to those obtained directly after calcination and all exchanged forms were identified as well crystalline and pure material possessing MWW topology (Fig. 3). It evidences that ion-exchange process did not result in a structural transformation of MCM-22.

SEM pictures of the ion-exchanged MCM-22 samples slightly differ from the images of MCM-49 exchanged samples. While the crystals of K and Cs-exchanged MCM-22

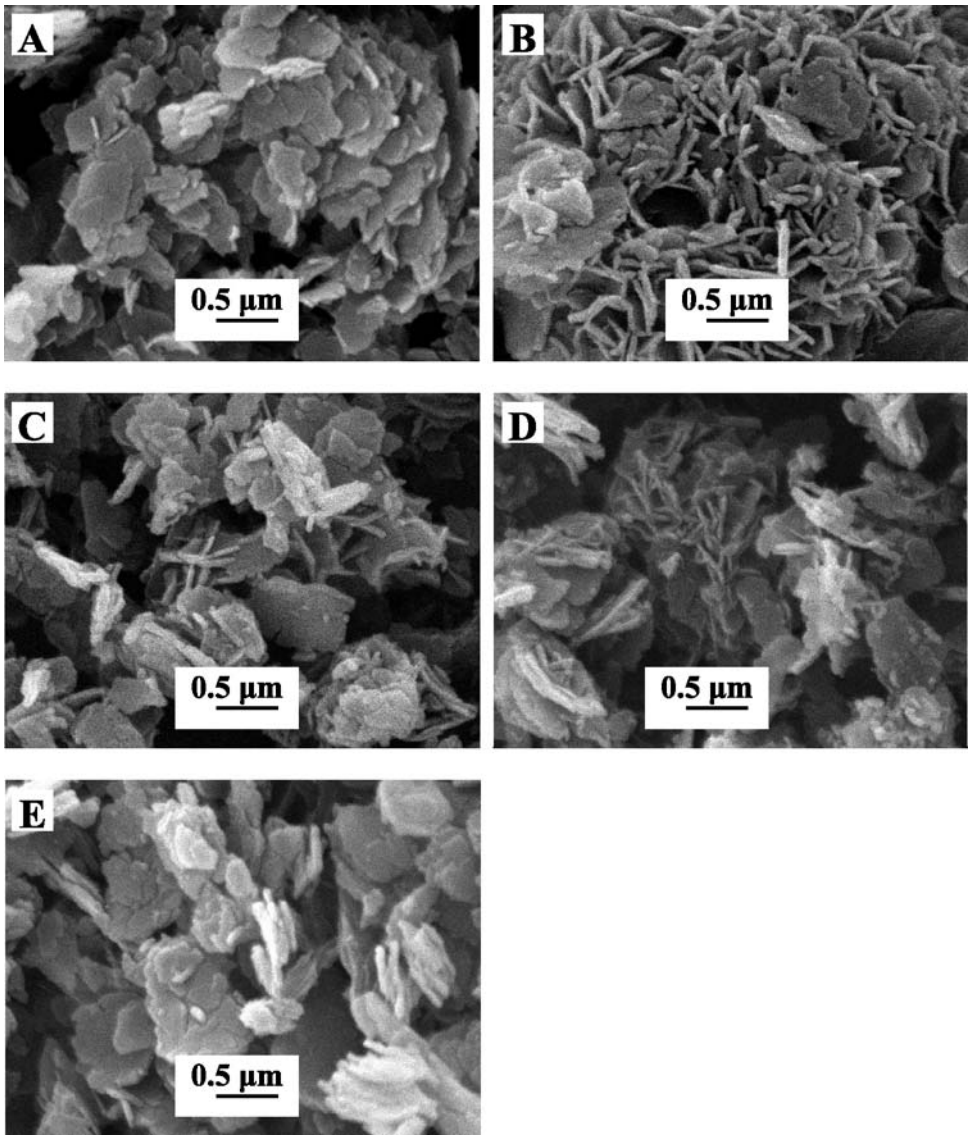

Fig. 2 Scanning electron micrographs of MCM-22 with different initial Si/Al: **A** 15, **B** 20, **C** 30, **D** 40 and **E** MCM-49 with initial Si/Al = 15

samples form almost spherical aggregates, the morphology of the crystals of MCM-49 samples was preserved in all modified samples (Fig. 4).

The degree of the ion exchange increased with increasing Si/Al molar ratio in the MWW materials (Table 2). The highest degree of ion exchange was achieved for Na^+ forms (ca. 80%). For K^+ forms the exchange was incomplete and it decreased stronger for Li^+ and Cs^+ forms. The individual positions of alkali-metal exchanged MCM-22 and MCM-49 were not yet determined. Thus, we can only speculate that some cationic positions are more or less specific for individual cations, which is known, e.g. in ferrierite (Nachtigall and Bulánek 2006).

The nitrogen isotherms obtained for MCM-22/MCM-49 zeolites are shown in Figs. 5 and 6. The BET surface areas, which agree well with the literature data (Rodriguez et al. 2000; Corma et al. 2001; Laforge et al. 2005), are summarized in the Table 3. The surface area of MCM-22 zeolites decreases with the increasing the Si/Al ratio. The surface area of the Na-MCM-22/15 sample (542 m^2/g) slightly differs from that of Na-MCM-49/15 (490 m^2/g). It can be seen from the data in Table 3 that the surface area the MWW materials decreases significantly after cation exchange in the order of increasing weight of alkali metal cations. The only exception is the case of Li^+ form of MCM-22; the relatively large decrease in the surface area could be caused by a decrease in the crystallinity as might indicate the X-ray diffractogram in Fig. 3A.

All nitrogen isotherms recorded on MWW samples show an H4 type hysteresis loop according to the IUPAC classification (Lowell et al. 2004). This type of hysteresis loop is usually related to slit-shaped pores among plateled particles, which is the case of MCM-22 samples (Fig. 2). The isotherms on MCM-22 and MCM-49 are very similar,

Table 2 Chemical analysis of the MWW zeolites after ion-exchange modification with different cations

Parent	Zeolite	Si/Al (XRF)	M/Al (XRF)
S003	Na-MCM-22/15	13.5	0.83
S004	Na-MCM-22/20	19.2	0.85
S005	Na-MCM-22/30	30	0.92
S006	Na-MCM-22/40	39.2	0.94
S001	Li-MCM-22/15	14.4	0.56
S001	K -MCM-22/15	14.7	0.65
S001	Cs-MCM-22/15	14.2	0.53
S006	Li-MCM-22/40	39.6	0.58
S006	K-MCM-22/40	40.2	0.85
S006	Cs-MCM-22/40	39.6	0.55
S004	K-MCM-22/20	20.5	0.76
S005	K-MCM-22/30	31.6	0.91
S008	Li-MCM-49/15	11.4	0.56
S008	Na-MCM-49/15	11.6	0.75
S008	Cs-MCM-49/15	12.0	0.47

Table 3 Textural characteristic of the alkali cation exchanged MWW materials

Zeolite	Surface area		Pore volume	
	S_{total} [m^2/g]	$S_{external}$ [m^2/g]	V_{total} [cm^3/g]	V_{micro} [cm^3/g]
Na-MCM-22/15	542	145	0.54	0.17
Na-MCM-22/20	506	139	0.47	0.18
Na-MCM-22/30	481	99	0.38	0.19
Na-MCM-22/40	329	84	0.30	0.12
Li-MCM-22/15	466	140	0.52	0.16
K -MCM-22/15	479	141	0.53	0.17
Cs-MCM-22/15	423	133	0.47	0.14
Li-MCM-22/40	316	86	0.31	0.11
K-MCM-22/40	338	86	0.33	0.12
Cs-MCM-22/40	294	79	0.28	0.10
K-MCM-22/20	473	135	0.46	0.16
K-MCM-22/30	449	98	0.39	0.17
Li-MCM-49/15	476	103	0.43	0.18
Na-MCM-49/15	490	106	0.44	0.19
Cs-MCM-49/15	391	92	0.35	0.15

showing a marked hysteresis at high p/p_o values, indicating small zeolite crystals (Figs. 5 and 6). The total pore volume was calculated from the amount of nitrogen adsorbed at $p/p_0 \approx 0.99$, the micropore volume and the external surface area were determined using the t-plot method. The values of the external surface area correspond to the small size of the zeolite particles. The values of micropore volume decrease after cation exchange, which is analogous to the changes of the BET surface area.

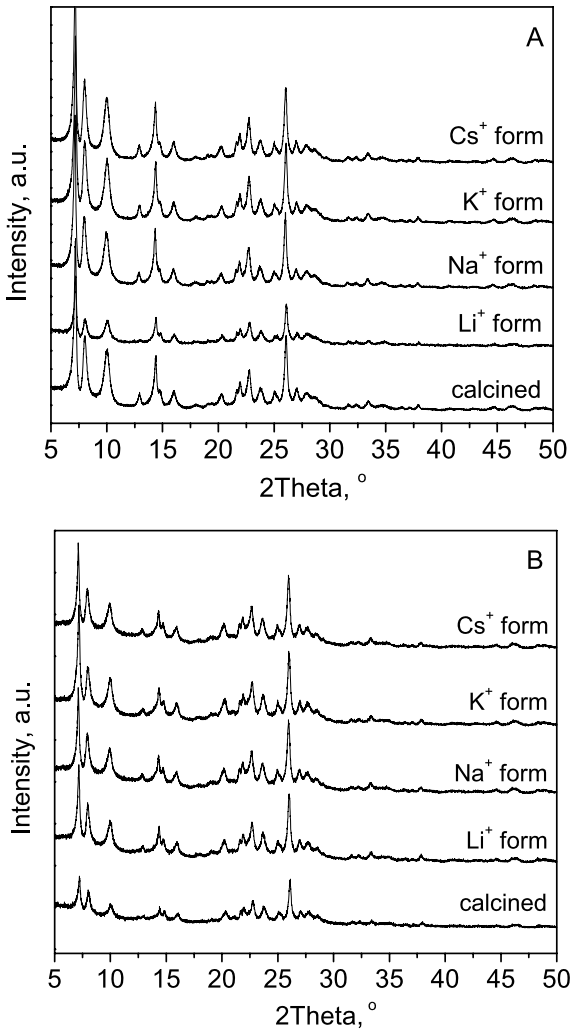

Fig. 3 X-ray diffraction of (**A**) MCM-22 and (**B**) MCM-49 samples with initial Si/Al = 15 after ion-exchange modification with different cations

For MCM-22/MCM-49 zeolites adsorption isotherms of carbon dioxide at 0°C exhibit nonlinear concave decreasing course, which is typical for strong interactions between CO_2 and cations. Figure 7A shows carbon dioxide adsorption isotherms on Na^+ form of MCM-22 zeolite compared with those obtained on zeolite MCM-49. Figure 7B presents the dependence of adsorption capacity of CO_2 on the content of K^+ in MCM-22 with different Si/Al ratios. The clear decrease in the adsorption capacities is observed for MCM-22 with the initial Si/Al molar ratio equal 40. The samples with Si/Al molar ratio in the range from 15 to 30 show almost the same adsorption capacities. The highest CO_2 adsorption capacity, obtained on the Na-MCM-49/15 with Si/Al ratio of 15 reveals the influence of the cation content on the adsorption ability. As the type of cation influences both the electric field inside the pores and the available pore volume, the materials with high cation content show clear dependence of CO_2 adsorption on the cation nature (Fig. 8). The lowest ad-

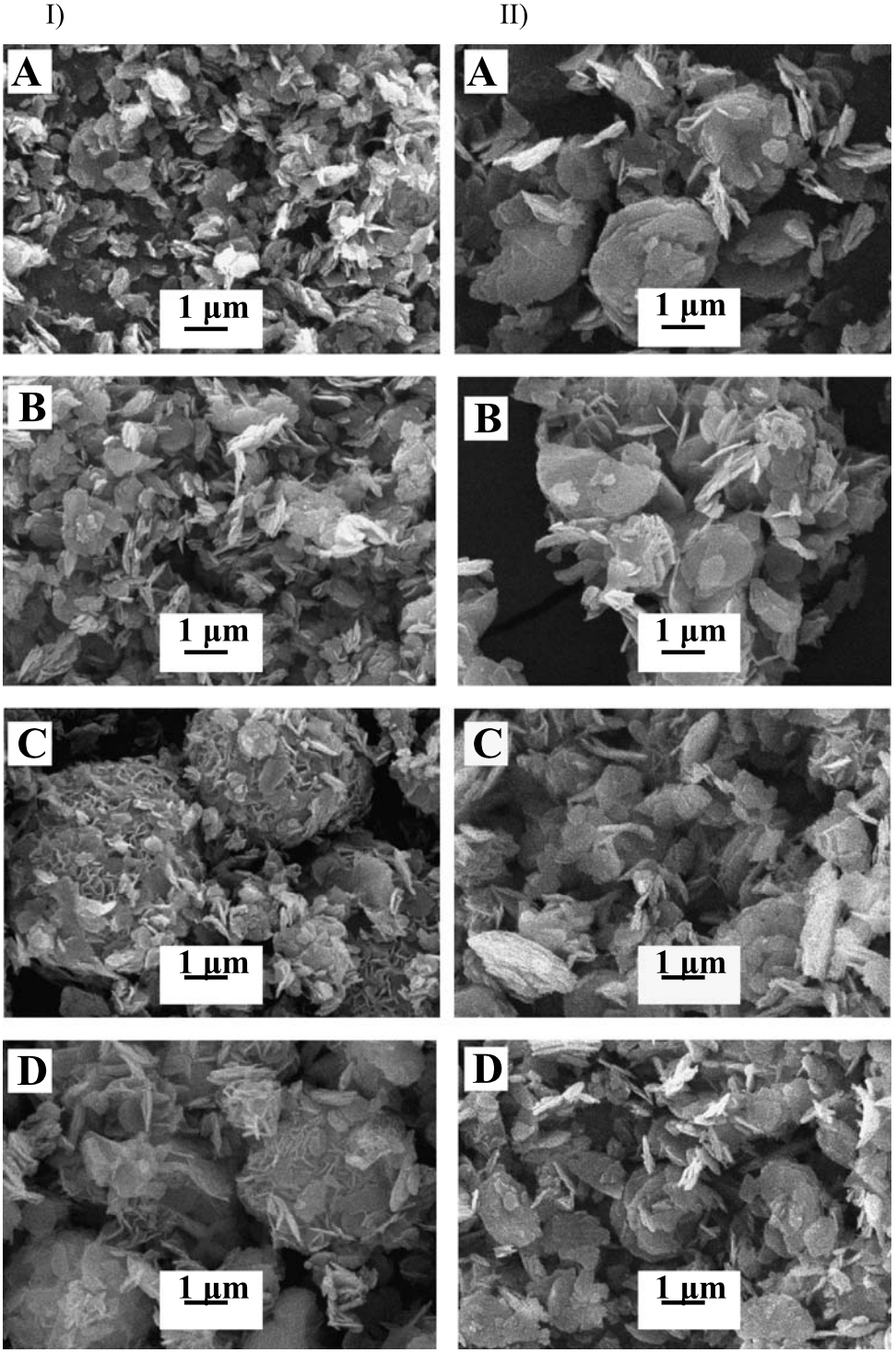

Fig. 4 Scanning electron micrographs of (**I**) MCM-22 and (**II**) MCM-49 zeolites with initial Si/Al = 15, after ion-exchange modification with different cations: **A** = Li^+, **B** = Na^+, **C** = K^+, **D** = Cs^+

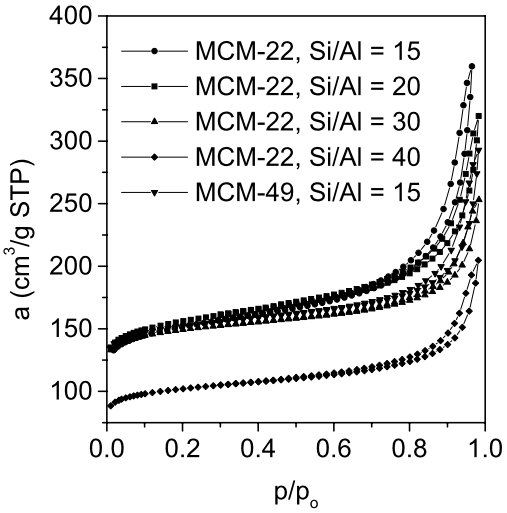

Fig. 5 Nitrogen adsorption isotherms of Na-MWW zeolite with different Si/Al molar ratios

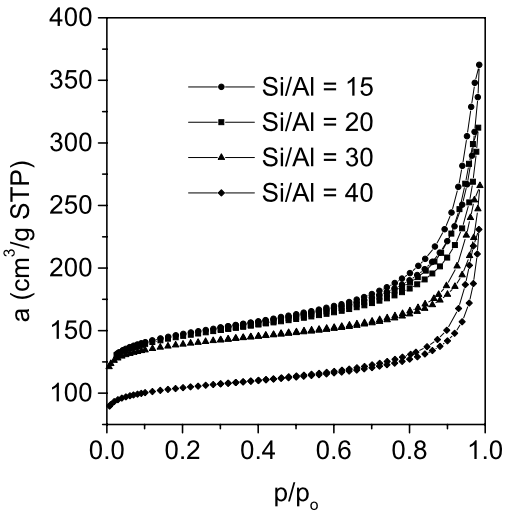

Fig. 6 Nitrogen adsorption isotherms of MCM-22 zeolite with different initial Si/Al after ion exchange modification with K^+

sorption capacities were obtained for materials containing the largest Cs^+ cations.

The slope of the CO_2 isotherms (i.e. Henry's constant $K_H = a/(p/p_0)$ in the low pressure region of $p/p_0 < 5 \cdot 10^{-4}$ is influenced by the nature of cations (Table 4). With exception of the sample K-MCM-22/15 it can be observed the similar tendency as in the case of NaX faujasites (Walton et al. 2006). The constant K_H attains the largest values for the Li^+ and Cs^+ forms of MCM-22 and MCM-49; the smallest ones are obtained for Na^+ forms.

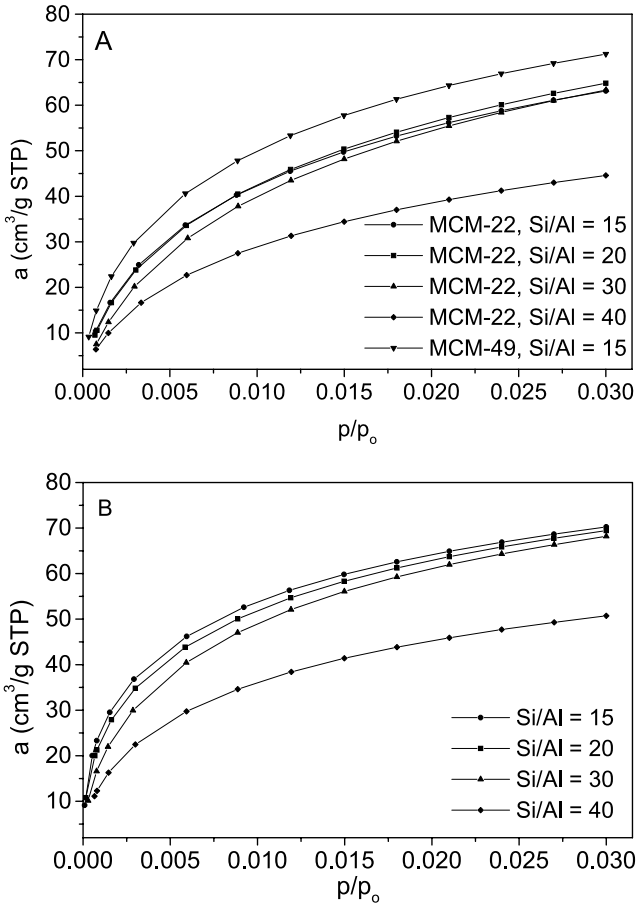

Fig. 7 Carbon dioxide adsorption isotherms of (**A**) MWW zeolite with different Si/Al molar ratios and (**B**) MWW zeolite with different initial Si/Al after ion exchange modification with K^+

4 Conclusions

MCM-22 and MCM-49 zeolites were synthesized and exchanged with Li^+, Na^+, K^+, and Cs^+ cations. All prepared materials were characterized using powder X-ray diffraction, scanning electron microscopy, X-ray fluorescence spectroscopy, and nitrogen adsorption at −196°C. Adsorption equilibrium data were measured on all materials at 0°C up to 101 kPa. The experimental results clearly reveal the dependence of CO_2 adsorption on the amount and nature of cations. The highest CO_2 adsorption capacity was obtained on the Na-MCM-49/15 with Si/Al ratio of 15, the lowest adsorption capacities were obtained for materials containing the largest Cs^+ cations.

Acknowledgements This work was supported by EU (DeSSANS, SES6-CT-2005-020133). J.P. thank EU for Marie Curie PhD position in the project 'INDENS' (MRTN-CT-2004-005503). The authors thank CS Cabot Corporation (Valašské Meziříčí, Czech Republic) for providing Cab-O-Sil M5. We also thank Dr. L. Brabec (J. Heyrovský Institute of Physical Chemistry, v.v.i., Academy of Sciences of the Czech Republic) for recording SEM images.

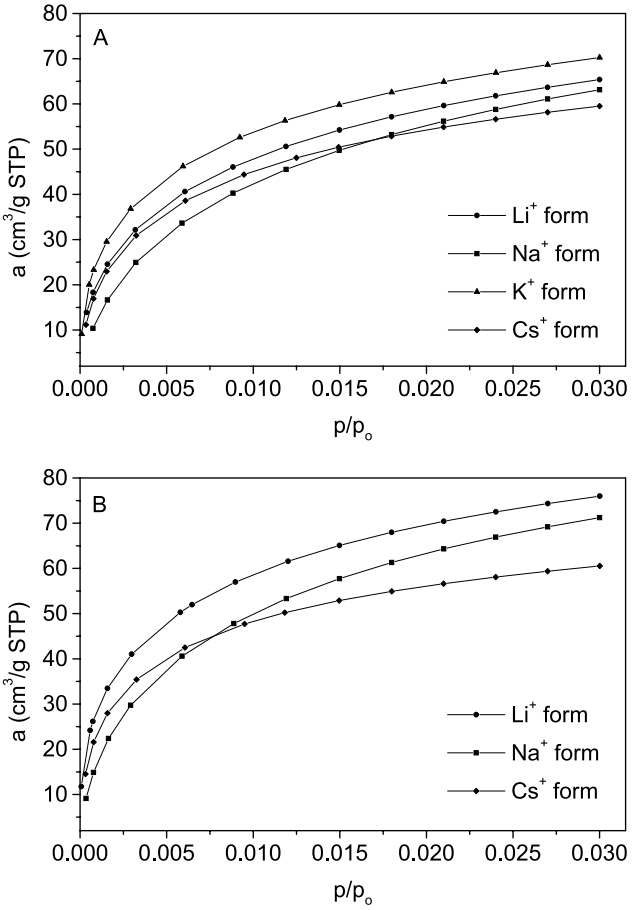

Fig. 8 Carbon dioxide adsorption isotherms of (**A**) MCM-22 zeolite with initial Si/Al = 15 after ion-exchange modification and (**B**) MCM-49 zeolite with initial Si/Al = 15 after ion-exchange modification

Table 4 The Henry's constants K_H for CO_2 adsorption isotherms on ion-exchanged MCM-22 and MCM-49 zeolites

Zeolite	$10^{-3} K_H$ [cm³/g STP]
Li-MCM-22/15	30.7
Na-MCM-22/15	14.0
K-MCM-22/15	38.8
Cs-MCM-22/15	26.6
Li-MCM-49/15	44.3
Na-MCM-49/15	22.4
Cs-MCM-49/15	34.7

References

Barrett, P.A., Díaz-Cabañas, M.-J., Camblor, M.A.: Crystal structure of zeolite MCM-35 (MTF). Chem. Mater. **11**, 2919–2927 (1999)

Čejka, J., Krejčí, A., Žilková, N., Kotrla, J., Ernst, S., Weber, A.: Activity and selectivity of zeolites MCM-22 and MCM-58 in the alkylation of toluene with propylene. Microporous Mesoporous Mater. **53**, 121–133 (2002)

Čejka, J., Wichterlová, B.: Catal. Rev. **44**, 375–421 (2002)

Corma, A., Corell, C., Pérez-Pariente, J.: Synthesis and characterization of the MCM-22 zeolite. Zeolites **15**, 2–8 (1995)

Corma, A., Fornes, V., Galletero, M.S., Garcia, H., Gomez-Garcia, C.J.: Prevalence of the external surface over the internal pores in the spontaneous generation of tetrathiafulvalene radical cation incorporated in the novel delaminated ITQ-2 zeolite. Phys. Chem. Chem. Phys. **3**, 1218–1222 (2001)

Corma, A., Martínez-Triguero, J.: The use of MCM-22 as a cracking zeolitic additive for FCC. J. Catal. **165**, 102–120 (1997)

Delaval, Y., De Lara, E.C.: Study of physisorption of carbon dioxide on NaA zeolite. J. Chem. Soc., Faraday Trans. 1 **77**, 869–877 (1981)

Dorset, D.L.: Electron crystallography of zeolites. 3. Calcined MCM-22 and MCM-49, a case of subtle differences. Z. Kristallogr. **218**, 612–616 (2003)

Dorset, D.L., Roth, W.J., Gilmore, C.J.: Electron crystallography of zeolites—the MWW family as a test of direct 3D structure determination. Acta Cryst. **A61**, 516–527 (2005)

Kennedy, G.J., Lowton, S.L., Fung, A.S., Rubin, M.K., Steuernagel, S.: Multinuclear MAS NMR studies of zeolites MCM-22 and MCM-49. Catal. Today **49**, 385–399 (1999)

Kučera, J., Nachtigall, P., Kotrla, J., Košová, G., Čejka, J.: Pyrrole as a probe molecule for characterization of basic sites in ZSM-5: a combined FTIR spectroscopy and computational study. J. Phys. Chem. B **108**, 16012–16022 (2004)

Laforge, S., Ayrault, P., Martin, D., Guisnet, M.: Acidic and catalytic properties of MCM-22 and MCM-36 zeolites synthesized fro the same precursors. Appl. Catal. A **279**, 79–88 (2005)

Lawton, S.L., Fung, A.S., Kennedy, G.J., Alemany, L.B., Chang, C.D., Hatzikos, G.H., Lissy, D.N., Rubin, M.K., Timken, H.-K.C., Sterernagel, S., Woessner, D.E.: Zeolite MCM-49: a three dimensional MCM-22 analogue synthesized by in situ crystallization. J. Phys. Chem. **100**, 3788–3798 (1996)

Leonowicz, M.E., Lowton, J.A., Rubin, M.K.: MCM-22: A molecular sieve with two independent multidimensional channel systems. Science **264**, 1910–1913 (1994)

Lowell, S., Shields, J.E., Thomas, M.A., Thommes, M.: Characterization of Porous Solids and Powders: Surface Area, Pore Size and Density, p. 44. Kluwer, Dordrecht (2004)

Maurin, G., Llewellyn, P.L., Poyet, Th., Kuchta, B.: Adsorption of argon and nitrogen in X-faujasites: relationships for understanding the interactions with monovalent and divalent cations. Microporous Mesoporous Mater. **79**, 53–59 (2005)

Nachtigall, P., Bulánek, R.: Theoretical investigation of site-specific characteristics of CO adsorption complexes in the Li^+-FER zeolite. Appl. Catal. A **307**, 118–127 (2006)

Plant, D.F., Maurin, G., Deroche, L., Gaberova, L., Llewellyn, P.L.: CO_2 adsorption in alkali cation exchanged Y faujasites: a quantum chemical study compared to experiments. Chem. Phys. Lett. **426**, 387–392 (2006)

Ravishankar, R., Sivasanker, S.: Hydroisomerization of n-hexane over Pt-H-MCM-22. Appl. Catal. A **142**, 47–59 (1996)

Rodriguez, I., Climent, M.J., Iborra, S., Fornes, V., Corma, A.: Use of delaminated zeolites (ITQ-2) and mesoporous molecular sieves in the production of fine chemicals: preparation of dimethylacetals and tetrahydropyranylation of alcohols and phenols. J. Catal. **192**, 440–447 (2000)

Roth, W.J.: MCM-22 zeolite family and the delaminated zeolite MCM-56 obtained in one-step synthesis. Stud. Surf. Sci. Catal. **158**, 19–26 (2005)

Rubin, M.K., Chu, P.: U.S. patent 4,954,325 (1990)

Santos Marques, A.L., Fontes Monteiro, J.L., Pastore, H.O.: Static crystallization of zeolites MCM-22 and MCM-49. Microporous Mesoporous Mater. **32**, 131–145 (1999)

Shiralkar, V.P., Kulkarni, S.B.: Sorption of carbon dioxide in cation exchanged Y type zeolites: sorption isotherms and state of sorbed molecule. Zeolites **4**, 329–336 (1984)

Siriwardane, R.V., Shen, M.-S., Fisher, E.P., Poston, J.A.: Adsorption of CO_2 on molecular sieves and activated carbon. Energy Fuels **15**, 279–284 (2001)

Tanabe, K., Hölderich, W.F.: Industrial application of solid acid-base catalysts. Appl. Catal. A **181**, 399–434 (1999)

Walton, K.S., Abney, M.B., LeVan, M.D.: CO_2 adsorption in Y and X zeolites modified by alkali metal cation exchange. Microporous Mesoporous Mater. **91**, 78–84 (2006)